Hot-phonon generation in GaAs/$Al_xGa_{1-x}As$ superlattices: Observations and implications on the coherence length of LO phonons

D. S. Kim, A. Bouchalkha, J. M. Jacob, and J. J. Song
Department of Physics and Center for Laser Research, Oklahoma State University, Stillwater, Oklahoma 74078

J. F. Klem
Sandia National Laboratories, Albuquerque, New Mexico 87185

H. Hou and C. W. Tu
Department of Electrical Engineering, University of California at San Diego, La Jolla, California 92093

H. Morkoç
Coordinated Science Laboratory, University of Illinois at Urbana-Champaign, Urbana, Illinois 61801
(Received 3 March 1994; revised manuscript received 3 June 1994)

Using picosecond Raman scattering, hot-phonon occupation numbers (N) of GaAs and GaAs-like LO phonons have been studied over a wide range of structural parameters in more than 30 GaAs/$Al_xGa_{1-x}As$ superlattices. In addition, simultaneous measurements of these LO phonon modes in bulk GaAs and $Al_xGa_{1-x}As$ alloys are made for comparison. N values of both GaAs and GaAs-like modes of the superlattices are comparable to or larger than those of bulk GaAs or $Al_xGa_{1-x}As$ alloys for $x<0.2$. On the other hand, N values of GaAs or GaAs-like LO phonons are much smaller for $x>0.35$, unless the barrier widths are very thin (<15 Å). The implications of our results on spatial properties of LO phonons are discussed and compared with relevant theoretical and experimental studies.

Spatial properties (or coherence lengths) of LO phonons in GaAs/$Al_xGa_{1-x}As$ superlattices (SL's) as a function of x or layer thicknesses have attracted some attention over the last decade.[1-15] There is now general agreement that an infinite-barrier picture can be used for LO phonons in GaAs/AlAs superlattices because of the relatively large energy separation (≈ 100 cm^{-1}) between the optical phonons in GaAs and AlAs.

While phonon properties of GaAs/AlAs SL's have been extensively studied using Raman scattering,[16-18] those of GaAs/$Al_xGa_{1-x}As$ SL's are more complicated because of the two-moded behavior of optical phonons in $Al_xGa_{1-x}As$ alloys. In GaAs/$Al_xGa_{1-x}As$ SL's, GaAs and GaAs-like LO phonons are much more likely to be bulklike and propagating compared with LO phonons in GaAs/AlAs SL's. This is because GaAs-like LO phonons of $Al_xGa_{1-x}As$ lie very close in energy to GaAs LO phonons, so that the barrier height in GaAs/$Al_xGa_{1-x}As$ SL's for $x<0.3$ is much smaller (for instance, ≈ 10 cm^{-1} or less for $x<0.3$).

In this paper, we have measured N for GaAs LO phonons by picosecond Raman scattering in over 30 molecular-beam-epitaxy grown SL's with various x ($0.10 \le x \le 1$), well width L_z ($70 \le L_b \le 150$ Å), and barrier width L_b ($5 \le L_b \le 150$ Å) at 20 K. The laser mainly used was the second harmonic of a mode-locked Nd:YAG (yttrium aluminum garnet) laser (2.33 eV, 1.5 ps), as well as a synchronously pumped dye laser (1.9–2.1 eV, 1.5 ps). With these exciting photon energies, hot-electron relaxation that generates hot phonons occurs mostly above the alloy barrier in most of the samples investigated. N was found to be sensitive to both x and L_b: when $x \le 0.2$, bulklike occupation numbers for both GaAs and the GaAs-like LO phonons are observed in all ranges of L_b and L_z, while when $x>0.35$, N values of GaAs LO phonons are much smaller when $L_b>15$ Å, typically at 10–20% that of bulk GaAs. These small values are comparable to those of a GaAs/AlAs SL ($L_z=L_b=100$ Å), where LO phonons are believed to be perfectly confined. When the barriers are very thin (<15 Å), a bulklike N is again recovered even for $x>0.35$. These results can be summarized in a two-dimensional phase diagram (Fig. 3) where regions of bulklike N and the (GaAs/AlAs SL)-like N are well separated in the two-dimensional phase diagram of x and L_b. Our results can be explained qualitatively (and also somewhat quantitatively, see Fig. 4) if we assume that the confined Raman-active LO phonons in the well eventually become propagating and Bloch wave functionlike, with their coherence length ξ much larger than the well widths. This interpretation is in good agreement with some of the recent theoretical studies.[7-10]

In Fig. 1(a), the Stokes and anti-Stokes Raman spectra of GaAs and GaAs-like LO phonons of a GaAs/$Al_{0.2}Ga_{0.8}As$ SL ($L_x=L_b=70$ Å, 20 periods) at 20 K are plotted. GaAs and GaAs-like modes of the GaAs/$Al_{0.2}Ga_{0.8}As$ superlattice are reasonably well resolved with a separation of ≈ 7 cm^{-1}. By comparing the Raman intensities around ± 295 and ± 288 cm^{-1}, or by deconvoluting the spectra, N values of both GaAs and

GaAs-like modes are obtained. Resonant Raman corrections in obtaining N are relatively small in our samples due to the off-resonance excitation conditions used. Both of these modes have values of N that are only slightly smaller than that of bulk GaAs also in the same cryostat and *larger* than that of $Al_{0.2}Ga_{0.8}As$. Therefore, from the point of view of hot-phonon generation, both GaAs and GaAs-like LO phonons in this SL are essentially bulklike when $x=0.2$.

In Fig. 1(b), the Stokes and anti-Stokes Raman spectra of GaAs and GaAs-like LO phonons of a $GaAs/Al_{0.4}Ga_{0.6}As$ SL ($L_x=100$ Å, $L_b=50$ Å, 30 periods) at 20 K are plotted. In this sample, the barrier height is ≈ 15 cm^{-1}, as can be readily seen from the Stokes Raman spectrum. N values of both GaAs and GaAs-like LO phonons are much smaller than those of bulk GaAs or the $GaAs/Al_{0.2}Ga_{0.8}As$ SL, but is comparable to that of a GaAs/AlAs SL with $L_x=L_b=100$ Å. Thus, N values of both GaAs and GaAs-like LO phonons in this SL are confined phononlike.

Because of the relatively low power densities ($<10^{17}$ cm^{-3}) we used, N is much less than 1 and linear with the laser power P. Therefore, experimental errors are reduced by comparing the normalized hot-phonon generation efficiency dN/dP between SL's and bulk GaAs instead of comparing N. In Fig. 2, the normalized (to bulk GaAs) hot-phonon generation efficiency dN/dP for

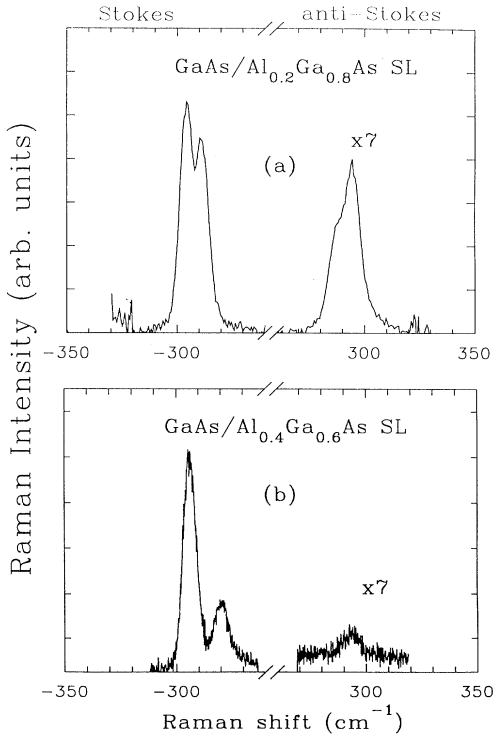

FIG. 1. The Stokes and anti-Stokes Raman spectra of GaAs and GaAs-like LO phonons (a) in a $GaAs/Al_{0.2}Ga_{0.8}As$ SL ($L_z=L_b=70$ Å, 20 periods) sample, and (b) in a $GaAs/Al_{0.4}Ga_{0.6}As$ ($L_z=100$ Å, $L_b=50$ Å, 30 periods) SL. Both samples are measured under identical conditions, together with bulk GaAs.

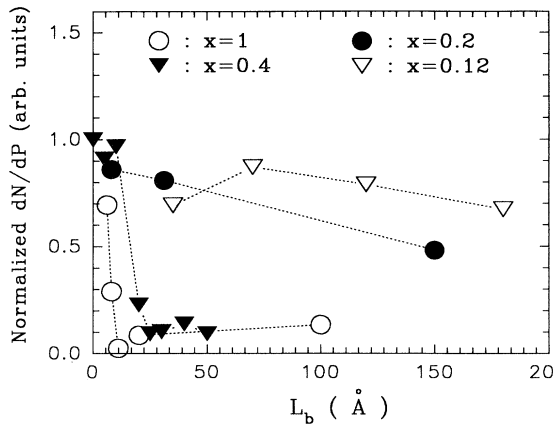

FIG. 2. Hot-phonon generation efficiency normalized to GaAs, plotted as a function of L_b for $x=1$ (empty circle), $x=0.4$ (filled inverted triangle), $x=0.2$ (filled circle), and $x=0.12$ (empty inverted triangle). Broken lines are a guide to the eye.

GaAs LO phonons of SL's are plotted against L_b for four series of SL's ($x=1$, 0.4, 0.2, and 0.12) with fixed $L_z=100$ Å. There is a clear L_b-dependent transition from bulklike efficiencies to much smaller efficiencies in the two series with $x=0.4$ or 1. Only bulklike efficiencies, however, are observed for all L_b's in the two series with $x=0.2$ and 0.12. GaAs and GaAs-like peaks are well resolved in Raman spectra up to $x=0.2$ [Fig. 1(a)], whereas it is difficult to separate them when $x=0.12$ due to the finite-band width (6 cm^{-1}) of our picosecond pulses. Therefore, dN/dP for the $x=0.12$ series should be regarded as the averaged generation efficiency of GaAs and GaAs-like modes.

For most sample parameters in Fig. 2, the normalized generation efficiency is either bulklike ($dN/dP>0.6$) or comparable to those of GaAs/AlAs SL's ($dN/dP<0.2$). This holds true for other series not shown here as well. Therefore, we can easily visualize our results in a parameter space of x and L_b as a phase diagram (Fig. 3), where the line is a guide to the eye, around which N (or dN/dP) changes from bulklike values to confined phononlike values, or vice versa. For comparison, the differences between the energies of GaAs LO phonons (295 cm^{-1}) and the GaAs-like LO phonons, which act as barrier heights, are indicated for several x values in the upper part of Fig. 3. It is clear that when the barrier height is smaller than ≈ 10 cm^{-1} ($x\approx 0.3$), LO phonons become bulklike, at least from the point of view of hot-phonon generation. This critical barrier height (or critical x) of ≈ 10 cm^{-1} (or $x\approx 0.3$) is in good agreement with the theoretical results of Refs. 8 and 10. Furthermore, these results are in qualitative agreement with Ref. 13, where it was found that 1 ML of AlAs can stop the propagation of GaAs LO phonons into the adjacent GaAs layer, while they propagate through $Al_xGa_{1-x}As$ monolayers with small x's. From these discussions, it is clear that the confined-to-propagation (or small-to-large ξ) transition of LO phonons as an explanation of our results warrants some further consideration.

It should be noted that for samples with small L_b's (<20 Å) in Figs. 2 and 3, the decrease in the effective x, resulting from the diffusion of Al atoms,[19,20] might be non-negligible. Such decrease in effective x is expected to shift the phase diagram shown in Fig. 3 somewhat, without changing the overall interpretation.

In the following, we perform simple calculations that illustrate that the large increase in N as x or L_b become small can be explained, at least qualitatively, by the confined-to-propagation transition. In Fig. 4(a), a hot-phonon distribution curve at $t=1$ ps that results from the relaxation of hot electrons in bulk GaAs excited at $t=0$ by a δ-function pulse is shown, where the hot-phonon occupation number N_q of a phonon mode with a wave vector q is plotted against q.[21,22] In obtaining this curve, we assumed a parabolic band with an initial excess energy of hot electrons at 500 meV. An instantaneous thermalization was assumed and the intervalley scattering into X and L valleys was included.[22] All of the above assumptions or the specific values of the excess energy, electron–LO-phonon scattering times, or intervalley scattering times, can be relaxed without changing the overall hot-phonon distribution curve. This is essentially because the shape of the hot-phonon distribution curve is determined mostly by the energy-momentum conservation of electron–LO-phonon scattering (which explains the cutoff at small q) and the Fröhlich matrix element $1/q^2$ (which explains the rapid decrease in N_q with increasing q). Note that the peak of the hot-phonon distribution curve occurs nearly at $q\approx q_0$, which is the Raman-active wave vector of bulk GaAs ($\approx 9\times 10^5$ cm^{-1} at the backscattering geometry with photon energy of 2.33 eV). Thus in *bulk GaAs, we probe approximately the maximum occupation number of the hot-photon distribution curve.*

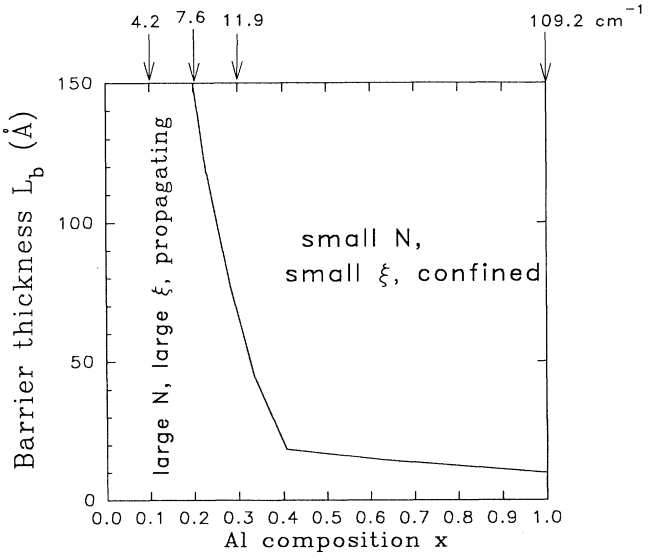

FIG. 3. A phase diagram of sample parameters x and L_b summarizing our results. The lines serve as a guide to the eye, around which N changes rather rapidly. The energy differences of GaAs and GaAs-like LO phonons are denoted as arrows for several x values on top of the figure.

We further assume that hot-electron relaxation in $GaAs/Al_xGa_{1-x}As$ SL's is bulklike. This drastic simplification is somewhat justified by the fact that the initial total excess energy (≈ 800 meV above the band gap) far exceeds the alloy barrier height for $0.2<x<0.3$ (roughly 200–300 meV). *We can then easily calculate the hot-phonon occupation number of an arbitrary phonon mode* simply by averaging the hot-phonon distribution curve of Fig. 4(a) weighed by the Fourier transform of the phonon wave function. We now show how phonon confinement and propagation can change the observed N. The Raman-active first confined LO-phonon mode can be represented by the following simple wave function and Fourier transform of it:

$$\Psi_c = \sin\frac{\pi z}{L_z}, \quad 0<z<L_z , \tag{1}$$

$$|F(q)|^2 = \frac{1+\cos(qL_z)}{\left[q^2-\frac{\pi^2}{L_z^2}\right]^2} . \tag{2}$$

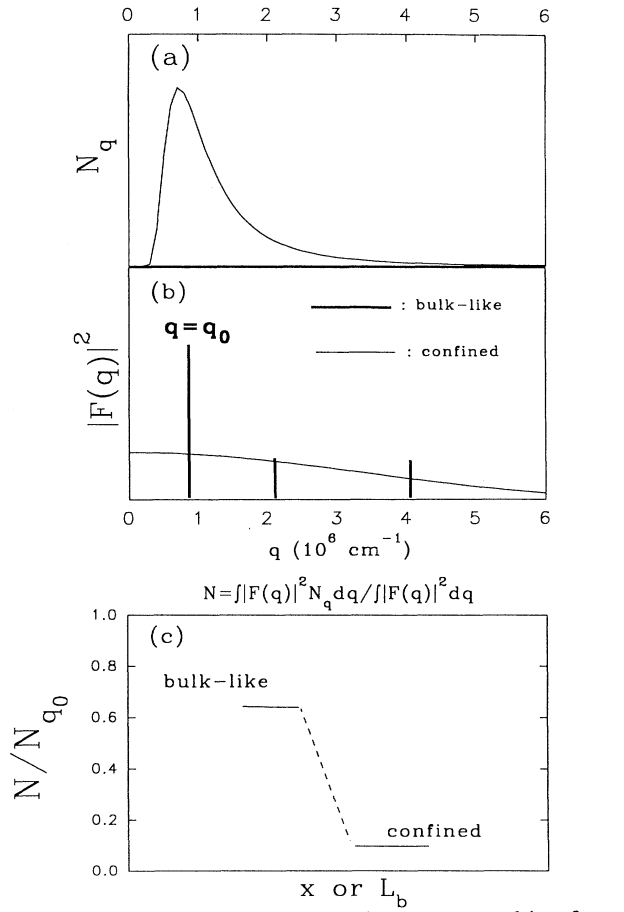

FIG. 4. (a) A hot-phonon distribution curve resulting from hot-electron relaxation in bulk GaAs calculated from Ref. 22. (b) Absolute square of the Fourier-transformed phonon wave function $|F(q)|$ for the Bloch wave function (thick lines) or the confined wave function [thin lines, from Eq. (2)] are shown. (c) A schematic diagram illustrating the change in N when a confined-to-propagation transition occurs, calculated from the results plotted in (a) and (b).

From Eq. (2) denoted by thin lines in Fig. 4(b) and the results of Fig. 4(a), we obtain the normalized N of 0.11 for the confined phonon of Eq. (1) [Fig. 4(c)]. Such a small N is a combined result of the relatively wide $|F(q)|^2$ of Eq. (2) resulting from small coherence length ξ of confined phonons, and the sharp decrease of N_q with increasing q. When phonons become propagating and thus can be represented by Bloch wave functions, the dominant Raman-active wave function off resonance can be represented by

$$\Psi_0 = \exp(iq_0 z)U(z) \ . \tag{3}$$

$U(z)$ is an even, periodic function with period of $L_z + L_b$. The Fourier transform $F(q)$ of this wave function would show a dominant peak at q_0 and weaker ones at $|q_0 \pm 2\pi/(L_z+L_b)|$, $|q_0 \pm 4\pi/(L_z+L_b)|$, ..., as shown with thick lines in Fig. 4(b) for $L_z = L_b = 100$ Å. For simplicity, we assume that $|F(q)|^2$ are 1 and 0.3 for q_0 and $|q_0 \pm 2\pi/(L_z+L_b)|$, respectively, and zero for the rest of the Fourier components. The resulting N is much larger than that of the confined phonon, at 65% of the bulk value N_q ($q = q_0$). This results directly from the fact that $|F(q)|$ peaks sharply at q_0 for the Bloch wave function of Eq. (3), so that bulklike N results [Fig. 4(c)]. It should be stressed that this bulklike N is not a result of choosing specific values for $|F(q)|^2$. Rather, any Bloch wave function of Eq. (3) with an even $U(z)$ is dominated by the bulk Raman-active Fourier component $q = q_0$ and, therefore, would result in bulklike N.

The calculations shown in Fig. 4, although simplistic, illustrate that the confined-to-propagating transition of LO phonons is certainly a feasible explanation for the bulklike N observed for small x and L_b. It should be noted that to observe bulklike, large N, it is not necessary to have such a well-defined Bloch wave function of Eq. (3). Rather, any $U(z)$ whose spatial extent is larger than $\pi/q_0 \approx 330$ Å would result in bulklike N, which is self-evident from our Fourier-transform arguments. Thus bulklike or propagating in the context of hot-phonon generation is somewhat relaxed (i.e., $\xi > 330$ Å) from the perfect Bloch wave function. Our hot-phonon technique and interpretation, compared with the theoretical and experimental cw Raman studies performed on thin SL samples,[11–13] provide a *complementary approach* to the problem of spatial properties of LO phonons. With its large dynamic range, which essentially stems from the rapidly changing hot-phonon distribution curve near the zone center, this technique can be particularly useful for most widely used quantum wells of ≈ 100 Å, where observation of multiple peaks is extremely difficult due to flat dispersion at the zone center.

Our phase diagram shown in Fig. 3, when interpreted as separating regions of confined or propagating LO phonons, is in good agreement with recent theoretical calculations of Colombo, Molteni, and Miglio, where a strong increase in theoretical Raman intensity for $x < 0.3$ in interpreted as the onset of propagating LO phonons.[8,10] Diagrammatic perturbative studies of Fertig and Reinecke are also in general agreement with our results and interpretation, although a change of LO-phonon properties with x is less abrupt in their studies. Furthermore, the existence of the critical alloy concentration x (≈ 0.3) might suggest that GaAs LO phonons in these SL's propagate via percolation.[23]

In conclusion, we have performed an extensive picosecond Raman-scattering study of LO phonons in $GaAs/Al_xGa_{1-x}As$ superlattices. Large, bulklike phonon occupation numbers are observed when $x \leq 0.2$ for all sample parameters, while much smaller values of N comparable to those of GaAs/AlAs SL's are observed for $x \geq 0.3$. These results can be qualitatively explained by assuming that LO phonons undergo confined-to-propagation (or small-to-large ξ) transition around $x \approx 0.2$–0.3. Our results are in good agreement with recent theoretical investigations.

We acknowledge helpful discussions with Professor P. Y. Yu and Professor M. Cardona. This work was supported at Oklahoma State University by the Office of Naval Research. The work at Sandia was supported by the Department of Energy under Contract No. DE-AC04-94AL85000.

[1] D. S. Kim and P. Y. Yu, in *Ultrafast Laser Probe Phenomena in Bulk and Microstructure Semiconductors,* edited by R. R. Alfano, SPIE Symposia Proceedings No. 1282 (SPIE, Bellingham, 1990), p. 39.
[2] D. S. Kim *et al.*, Phys. Rev. Lett. **68**, 1002 (1992).
[3] D. S. Kim *et al.*, Phys. Rev. Lett. **72**, 1572 (1994).
[4] G. S. Spencer and J. Menéndez, Phys. Rev. Lett. **72**, 1571 (1994).
[5] A. Kobayashi and A. Roy, Phys. Rev. B **35**, 2237 (1987).
[6] C. Colvard *et al.*, Phys. Rev. B **31**, 2080 (1985).
[7] H. A. Fertig and T. L. Reinecke, Phys. Rev. B **49**, 11 168 (1994).
[8] L. Colombo, C. Molteni, and L. Miglio, in *Proceedings of the 21st International Conference on the Physics of Semiconductors,* edited by P. Jiang and H. Z. Zheng (World Scientific, Singapore, 1992), pp. 777–780.
[9] F. Bechstedt *et al.*, Phys. Rev. B **47**, 13 540 (1993).
[10] C. Molteni, L. Colomb, L. Miglio, and G. Benedek, Phys. Rev. B **50**, 11 684 (1994).
[11] B. Jusserand and D. Paquet, Phys. Rev. B **30**, 6245 (1984).
[12] B. Jusserand *et al.*, Phys. Rev. Lett. **67**, 2803 (1991).
[13] B. Jusserand, D. Paquet, and F. Mollot, Phys. Rev. Lett. **63**, 2397 (1989).
[14] K. Huang and B. Zhu, Phys. Rev. B **38**, 13 377 (1988).
[15] B. K. Ridley, Phys. Rev. B **39**, 5282 (1989).
[16] B. Jusserand and M. Cardona, in *Light Scattering in Solids V,* edited by M. Cardona and G. Güntherodt, Topics in Applied Physics Vol. 66 (Springer, Berlin, 1989), p. 49 and references therein.
[17] A. K. Sood *et al.*, Phys. Rev. Lett. **54**, 2111 (1985).
[18] D. J. Mowbray *et al.*, Phys. Rev. B **43**, 1598 (1991).
[19] D. G. Deppe *et al.*, J. Appl. Phys. **64**, 1838 (1988).
[20] B. Jusserand *et al.*, Appl. Phys. Lett. **57**, 560 (1990).
[21] C. L. Collins and P. Y. Yu, Phys. Rev. B **30**, 4501 (1984).
[22] D. S. Kim and P. Y. Yu, Phys. Rev. B **43**, 4158 (1991).
[23] J. Jacob *et al.*, Solid State Commun. **91**, 721 (1994).